Photochemical & Photobiological Sciences

COMMUNICATION

Check for updates

Cite this: *Photochem. Photobiol. Sci.*, 2019, **18**, 309

Received 25th September 2018, Accepted 4th January 2019

DOI: 10.1039/c8pp00426a

rsc.li/pps

Efficient hydrogen production using photosystem I enhanced by artificial light harvesting dye†

Haruki Nagakawa, [a,b] Ayano Takeuchi,[a] Yuya Takekuma,[a,b] Tomoyasu Noji,‡[c] Keisuke Kawakami,[c] Nobuo Kamiya,[c] Mamoru Nango,[c] Rei Furukawa[d] and Morio Nagata *[a]

In this study, we improved the hydrogen production efficiency by combining photosystem I with an artificial light harvesting dye, Lumogen Red. In the reaction system, Lumogen Red allows light absorption and energy transfer to photosystem I by Förster resonance energy transfer; therefore, the Pt nanoparticles act as active sites for hydrogen generation.

Photosynthesis is used by plants and algae for the fixation of carbon dioxide and the conversion of solar energy into chemical energy.[1,2] Recent technological developments have led to increased consumption of fossil fuels, resulting in energy depletion and global warming.[3] Hence, much effort has been devoted to realizing artificial photosynthetic systems for the efficient utilization of solar energy.[4–6] As the fundamental step in this direction, the mechanism of photosynthesis in plants and algae has also been elucidated.[7–14] In plants and algae, photosystem I (PSI) and photosystem II (PSII), which are membrane protein complexes, are responsible for the light-driven reaction of photosynthesis. In this photosynthetic protein, the absorbed light energy is transferred from the light harvesting system to the reaction centre, and the quantum yield has been confirmed to be ~100%.[15] The electron transfer systems of PSI are highly aligned energetically and spatially.[16] Electron transfer from the lumenal side, which accepts electrons, to the stromal side, which donates electrons using the electron transfer system, enables physical charge separation and achieves high quantum yield.[17] Green algae present in polluted water bodies poses an environmental problem, but can produce both PSI and PSII. Therefore, energy generation using photosynthetic proteins has emerged as a hot topic of research in recent years.[18,19]

In artificial photosynthesis using semiconductors, since most of photocatalysts absorb ultraviolet light, the use of visible light is required for highly efficient photocatalytic reactions.[4] From this view point, PSI has an excellent feature of absorbing blue and red light in the visible light region. However, to increase the efficiency of artificial photosynthesis using PSI, it is required to utilize 450–650 nm light that can not be absorbed by PSI. Therefore, in this study, we attempted to combine hydrogen production system using PSI with the Förster Resonance Energy Transfer (FRET) concept used in dye-sensitized solar cells and photocatalytic hydrogen production.[20,21] In this system, an artificial light harvesting dye, Lumogen Red (LR) which can absorb visible light with wavelength of 490–630 nm was used as a donor for FRET. PSI acting as an acceptor is combined with a platinum (Pt) co-catalyst and generates hydrogen with the received energy. To the best of our knowledge, highly efficient hydrogen generation using PSI, together with energy harvesting by FRET, has not been reported previously, and our findings can serve as a guide for further improving the efficiency of devices based on photosynthetic proteins and for producing clean and sustainable energy (such as hydrogen).

PSI core complexes were purified from *Thermosynechococcus vulcanus* (*T. vulcanus*), according to the previous methods[22–24] with slight modifications. Harvested *T. vulcanus* cells were treated with lysozyme for 2 h at 38 °C in darkness and then centrifuged at 10 000*g* for 10 min. The obtained precipitants were suspended in a small amount of a buffer containing 25% (w/v) glycerol, 20 mM Hepes-NaOH (pH 7.0), and 10 mM $MgCl_2$. Subsequently, the samples were stored at −80 °C, and

[a]*Department of Industrial Chemistry, Graduate School of Engineering, Tokyo University of Science, 12-1 Ichigayafunagawara-cho, Shinjuku-ku, Tokyo, 162-0826, Japan. E-mail: 4218533@ed.tus.ac.jp, 4218528@ed.tus.ac.jp, 4218701@ed.tus.ac.jp, nagata@ci.kagu.tus.ac.jp*

[b]*Photocatalyst Group, Research and Development Department, Local Independent Administrative Agency Kanagawa Institute of industrial Science and TEChnology (KISTEC), Japan. E-mail: haruki.nagakawa@gmail.com*

[c]*The OCU Advanced Research Institute for Natural Science & Technology (OCARINA), Osaka City University, 3-3-138 Sugimoto, Sumiyoshi-ku, Osaka 558-8585, Japan. E-mail: tnoji@ocarina.osaka-cu.ac.jp, keikawa@sci.osaka-cu.ac.jp, nkamiya@sci.osaka-cu.ac.jp, nango@ocarina.osaka-cu.ac.jp*

[d]*The University of Electro-Communications, Chofugaoka 1-5-1, Chofu, Tokyo 182-8585, Japan. E-mail: furukawa@ee.uec.ac.jp*

†Electronic supplementary information (ESI) available. See DOI: 10.1039/c8pp00426a

‡Present address: Research Center for Advanced Science and Technology, The University of Tokyo, 4-6-1 Komaba, Meguro-ku, Tokyo 153-8904, Japan. E-mail: tnoji@protein.rcast.u-Tokyo.ac.jp

the thylakoid membranes were obtained by a freeze–thawing method.[25] The thylakoid membranes were solubilized with 0.6% (w/v) *n*-dodecyl-β-D-maltoside (β-DDM) and then centrifuged at 38 900*g* for 90 min at 4 °C. Next, the obtained supernatants were filtrated through a 0.45 μm filter and loaded onto an anion-exchange column (DEAE TOYOPEARL 650S) with 5% (w/v) glycerol, 30 mM Mes (pH 6.0), 3 mM $CaCl_2$, and 0.03% (w/v) β-DDM. The column was washed with the same buffer containing 80 mM NaCl to remove a large amount of phycobilisome impurities. PSI core complexes were eluted with a linear gradient of NaCl concentration from 80 to 140 mM in the same buffer. The fluorescence spectra of these core complexes were measured at 25 °C and −196 °C to confirm the existence of PSI (Fig. S1†). The PSI/Pt nanoparticle (PSI/PtNP) composite was fabricated by following the methods reported by Chen *et al.* and Utschig *et al.*[26,27] To prepare the PtNPs, 5 mL of 67.6 mM $NaBH_4$ was added to a mixture of 10 mL of 3.38 mM H_2PtCl_6 and 1 mL of 23.7 mM mercaptosuccinic acid. Then, 5 mL of the buffer solution with 0.512 mL of the PSI extract solution (7.11 μM PSI trimer) and 1.82 mL of 2 mM PtNP were mixed, and the mixture was allowed to stand in a cool, dark place for 12 h to obtain the PSI/PtNP composite. It is considered that the interaction between PSI and PtNP is mainly electrostatic in nature.[27]

Hydrogen evolution experiments were conducted in a vial bottle (23 mL) with Ar gas circulation. The PSI/PtNP composite solution and 4 mL of 1 mM LR solution in methanol were prepared in the reaction cell, and 0.211 g of ascorbic acid and 17.4 mg of dichloroindophenol (DCIP) sodium salt were added as the sacrificial reagent and the reaction mediator, respectively. Thereafter, buffer solution was added to bring the total volume to 12 mL.

A Xe lamp (CERMAX LX-300, ILC Technology), with a UV cut-off filter (λ > 420 nm) and bandpass filter (λ = 490–630 nm), was used as the visible-light source. Ar flow was stopped for 30 min to accumulate the evolving hydrogen, and a 0.1 mL aliquot of this gas was collected using a gas-tight syringe. The sample was injected into the gas chromatograph (GC-8A, Shimadzu) for detection of the evolved hydrogen.

Fig. 1 shows the relationship between the amount of hydrogen evolution and the reaction time with the prepared composites. The absorption spectra of the PSI (a) and LR (b) are shown in Fig. 2. The fluorescence spectrum of the LR is shown in Fig. 2(c). Fig. 1 shows clear hydrogen evolution in the case of the PSI/PtNP + LR system, and only a small amount of hydrogen was detected in the case of PSI/PtNP. This was probably because the light intensity of the Xe lamp was weak at the wavelength of ~680 nm and excited electrons were insufficient for hydrogen generation with absorption by the chlorophyll of PSI. Since the generation of hydrogen involves a two-electron reduction reaction, almost no hydrogen production was observed under such low absorption conditions in that it was deactivated before the excited electrons gathered.[28] On the other hand, using the PSI/PtNP + LR system, hydrogen generation was observed due to energy transfer by FRET (Fig. 3). The spectra shown in Fig. 2(b) and (c), the fluorescence wavelength of LR overlaps with the absorption wavelength of PSI, which is one of the requirements for FRET to occur. The energy obtained by the absorption of light in the vicinity of 580 nm facilitated LR transfer to the reaction centre of PSI. The excited electrons in PSI were collected in PtNP, and hydrogen was generated by two-electron reduction. In PSI/PtNP + LR, the hydrogen production rate became constant at 26.3 mol H_2 (mol PSI)$^{-1}$ h^{-1}. In the early stages of the reaction, the excited electrons were consumed by the reduction of Pt, as the hydrogen generation rate gradually increased until stable

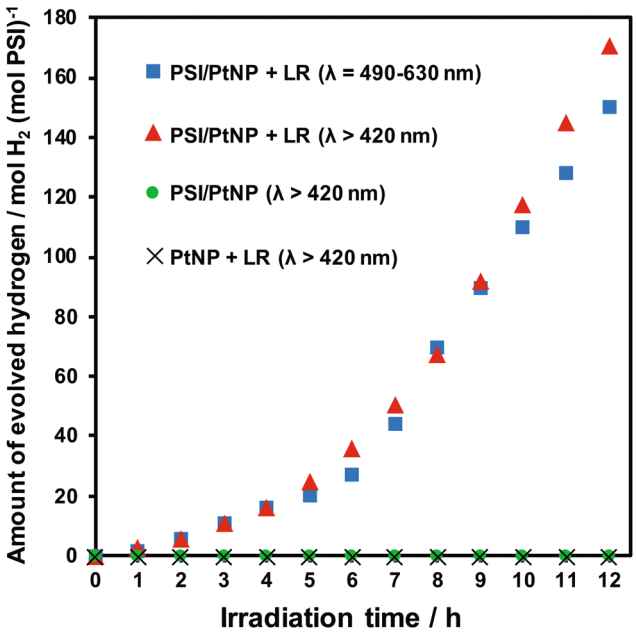

Fig. 1 Amount of evolved hydrogen as a function of time for the PSI/PtNP + LR and PSI/PtNP composites under visible light irradiation. Light source: Blue square, λ = 490–630 nm; red triangle, green circle and cross mark, λ > 420 nm; reactor: 23 mL vial bottle under Ar flow; reagents: ascorbic acid as a sacrificial reagent and DCIP as a mediator.

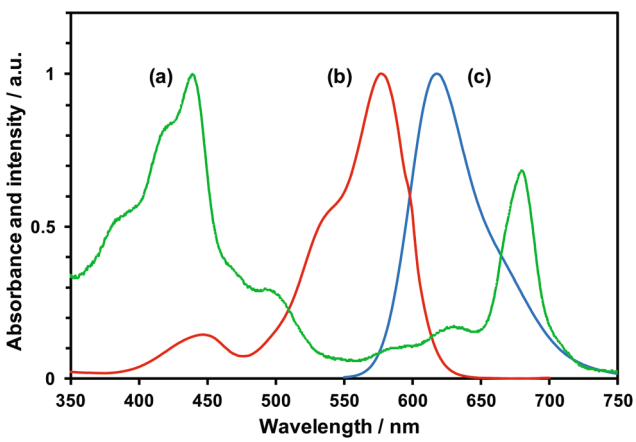

Fig. 2 (a) Absorption spectrum of the purified PSI in buffer solution after normalization. (b) Absorption spectrum of LR in methanol after normalization. (c) Fluorescence spectrum of LR in methanol after normalization.

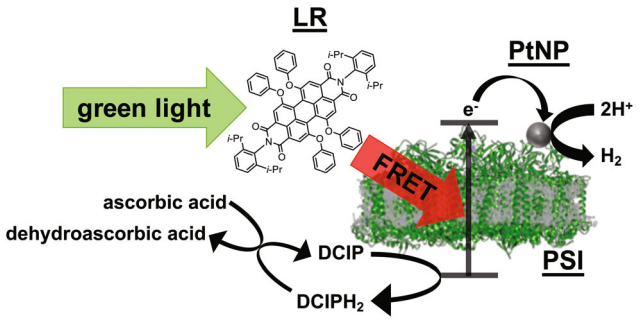

Fig. 3 Schematic illustration of the hydrogen evolution mechanism using the PSI/PtNP + LR composite in the presence of ascorbic acid as a sacrificial reagent and DCIP as a mediator.

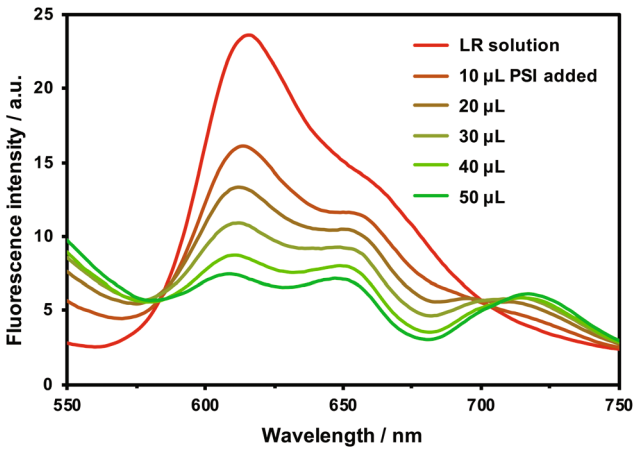

Fig. 4 Fluorescence quenching spectra of LR at different concentrations of PSI at 25 °C. Concentrations: [LR] = 6.67 μM, [PSI] = 2.04 mg chlorophyll per mL (adding from 10 to 50 μL).

hydrogen production was obtained. It was confirmed that a part of the prepared PtNP was oxidation state before the hydrogen evolution reaction from XPS analysis (Fig. S2†).

To confirm that hydrogen production is driven by the energy of light absorbed by LR, a hydrogen generation experiment was conducted using the absorption wavelength band of LR (λ = 490–630 nm) (Fig. 1, the plot of blue squares). The amount of generated hydrogen was almost same as that obtained using the cut-off filter (λ > 420 nm). This result suggests that hydrogen generation occurs mostly due to absorption of light of wavelength λ = 490–630 nm by LR. For confirming that the reaction follows the mechanism shown in Fig. 3, control experiments were performed with the same composite system but without PtNP or PSI; no hydrogen production was observed in either case. These results show that in the absence of LR, light absorption was insufficient for the two-electron reduction reaction to proceed. In the absence of PSI, hydrogen was not generated (Fig. 1, the plot of cross mark) because there was no energy acceptor, and the efficiency of charge separation was poor. In the absence of PtNP, no active sites were present for the hydrogen production reaction, and thus, hydrogen was not generated.

Furthermore, to confirm the energy transfer from LR to PSI, fluorescence quenching of LR upon adding PSI solution was experimentally studied, according to the following procedure. LR was dissolved in methanol to prepare a 0.02 mM solution. Thereafter, the prepared LR solution was diluted by adding Hepes-NaOH and 3 mL of the diluted solution was placed in the fluorescence measuring cell. The fluorescence spectra were upon excitation at 520 nm, and 10 μL of PSI solution (2.04 mg chlorophyll per mL) was added for each measurement, and finally a total of 50 μL was added. Fig. 4 shows that the fluorescence intensity of LR (near 620 nm) is attenuated by adding PSI solution. As the fluorescence of the donor molecule LR is quenched, the fluorescence intensity (near 720 nm) of PSI (as an acceptor) increases, which confirms that energy transfer by FRET occurs between PSI and LR. In addition, from the result of Fig. 4, we created a Stern–Volmer plot and obtained a linear approximation line (Fig. S3†). This fact suggests that quenching of LR fluorescence occurred by FRET.

In the hydrogen production system described here, LR absorbed visible light that cannot be absorbed by PSI (λ = 490–630 nm) and the energy transfer to PSI by FRET was realized. This fact is supported by the overlapping of the absorption spectrum of PSI and the fluorescence spectrum of LR (Fig. 2) and by the result that the fluorescence of LR was attenuated upon PSI addition and the fluorescence of PSI increased (Fig. 4 and Fig. S2†). The energy transferred from LR excites a special pair of electrons in PSI and the generated holes oxidize ascorbic acid *via* the DCIP mediator. On the other hand, the excited electrons move from the lumenal side to the stromal side of PSI, enabling highly efficient charge separation.[17] Thereafter, the excited electrons are collected at PtNPs organized on PSI. This facilitates two-electron reduction and the PtNPs behave as hydrogen evolution sites (Fig. 3). Hydrogen production under visible light can hardly be confirmed with PSI/PtNP, but due to the reaction following this mechanism, hydrogen generation could be observed (Fig. 1). This technique of using FRET to improve visible light absorption enabled taking advantage of the characteristics of PSI. In addition, it should be highly useful in the field of photochemistry in electrodes, solar cells, photocatalyst composites, *etc.*, for many applications such as hydrogen production, power generation, CO_2 reduction, *etc.*

Conclusions

In this study, PSI extracted from *T. vulcanus* was combined with PtNP and was used in combination with LR to archive hydrogen production in the presence of visible light. In the hydrogen generation reaction system described here, visible light, PSI, PtNP, and LR are all indispensable. LR absorbs visible light of sufficient energy and charge separation occurred at the reaction centre of PSI due to energy transfer from LR by FRET. The resultant excited electrons are collected in the composited PtNP, and hydrogen is evolved *via*

reduction. In the reaction system using light harvesting dye, the wavelength range for FRET can be extended, and it can be expected to be used for more efficient photocatalytic reactions and solar cells by choosing the appropriate light harvesting dye.

Conflicts of interest

There are no conflicts to declare.

Acknowledgements

The authors are grateful to Ryo Koyama and Ryota Yamauchi (Tokyo University of Science, Japan) for assistance with the experiments.

Notes and references

1 J. Barber, Biological solar energy, *Phil. Trans. R. Soc., A*, 2007, **365**, 1007–1023.
2 J. Barber, Photosynthetic Energy Conversion: Natural and Artificial, *Chem. Soc. Rev.*, 2009, **38**, 185–196.
3 *Climate Change 2007-the Physical Science Basis: Working Group I Contribution to the Fourth Assessment Report of the IPCC*, ed. S. Solomon, D. Qin, M. Manning, Z. Chen, M. Marquis, K. B. Averyt, M. Tignor and H. L. Miller, Cambridge university press, 2007, pp. 35–56.
4 A. Kudo and Y. Miseki, Heterogeneous Photocatalyst Materials for Water Splitting, *Chem. Soc. Rev.*, 2009, **38**, 253–278.
5 H. Nagakawa, T. Ochiai and M. Nagata, Fabrication of CdS/β-SiC/TiO_2 Tri-Composites that Exploit hole- and Electron-Transfer Processes for Photocatalytic Hydrogen Production under Visible Light, *Int. J. Hydrogen Energy*, 2018, **43**, 2207–2211.
6 H. Nagakawa, T. Ochiai, Y. Takekuma, S. Konuma and M. Nagata, Effective Photocatalytic Hydrogen Evolution by Cascadal Carrier Transfer in the Reverse Direction, *ACS Omega*, 2018, **3**, 12770–12777.
7 Y. Mazor, A. Borovikova and N. Nelson, The Structure of Plant Photosystem I Super-Complex at 2.8 A Resolution, *eLife*, 2015, **4**, e07433.
8 X. Pi, L. Tian, H. E. Dai, X. Qin, L. Cheng, T. Kuang, S. F. Sui and J. R. Shen, Unique Organization of Photosystem I-Light-Harvesting Supercomplex Revealed by Cryo-EM from a Red Alga, *Proc. Natl. Acad. Sci. U. S. A.*, 2018, **115**, 4423–4428.
9 X. Qin, M. Suga, T. Kuang and J. R. Shen, Structural Basis for Energy Transfer Pathways in the Plant PSI-LHCI Supercomplex, *Science*, 2015, **348**, 989–995.
10 X. Su, J. Ma, X. Wei, P. Cao, D. Zhu, W. Chang, Z. Liu, X. Zhang and M. Li, Structure and Assembly Mechanism of Plant $C_2S_2M_2$-Type PSII-LHCII Supercomplex, *Science*, 2017, **357**, 815–820.
11 M. Suga, F. Akita, M. Sugahara, M. Kubo, Y. Nakajima, T. Nakane, K. Yamashita, Y. Umena, M. Nakabayashi, T. Yamane, T. Nakano, M. Suzuki, T. Masuda, S. Inoue, T. Kimura, T. Nomura, S. Yonekura, L. J. Yu, T. Sakamoto, T. Motomura, J. H. Chen, Y. Kato, T. Noguchi, K. Tono, Y. Joti, T. Kameshima, T. Hatsui, E. Nango, R. Tanaka, H. Naitow, Y. Matsuura, A. Yamashita, M. Yamamoto, O. Nureki, M. Yabashi, T. Ishikawa, S. Iwata and J. R. Shen, Light-Induced Structural Changes and the Site of O=O Bond Formation in PSII Caught by XFEL, *Nature*, 2017, **543**, 131–135.
12 Y. Umena, K. Kawakami, J. R. Shen and N. Kamiya, Crystal Structure of Oxygen-Evolving Photosystem II at a Resolution of 1.9 Å, *Nature*, 2011, **473**, 55–60.
13 X. Wei, X. Su, P. Cao, X. Liu, W. Chang, M. Li, X. Zhang and Z. Liu, Structure of Spinach Photosystem II-LHCII Supercomplex at 3.2 Å Resolution, *Nature*, 2016, **534**, 69–74.
14 I. D. Young, M. Ibrahim, R. Chatterjee, S. Gul, F. Fuller, S. Koroidov, A. S. Brewster, R. Tran, R. A. Mori, T. Kroll, T. M. Clark, H. Laksmono, R. G. Sierra, C. A. Stan, R. Hussein, M. Zhang, L. Douthit, M. Kubin, C. de Lichtenberg, P. Long Vo, H. Nilsson, M. H. Cheah, D. Shevela, C. Saracini, M. A. Bean, I. Seuffert, D. Sokaras, T. C. Weng, E. Pastor, C. Weninger, T. Fransson, L. Lassalle, P. Brauer, P. Aller, P. T. Docker, B. Andi, A. M. Orville, J. M. Glownia, S. Nelson, M. Sikorski, D. Zhu, M. S. Hunter, T. J. Lane, A. Aquila, J. E. Koglin, J. Robinson, M. Liang, S. Boutet, A. Y. Lyubimov, M. Uervirojnangkoorn, N. W. Moriarty, D. Liebschner, P. V. Afonine, D. G. Waterman, G. Evans, P. Wernet, H. Dobbek, W. I. Weis, A. T. Brunger, P. H. Zwart, P. D. Adams, A. Zouni, J. Messinger, U. Bergmann, N. K. Sauter, J. Kern, V. K. Yachandra and J. Yano, Structure of Photosystem II and Substrate Binding at Room Temperature, *Nature*, 2016, **540**, 453–457.
15 N. Nelson, Plant Photosystem I – The Most Efficient Nano-Photochemical Machine, *J. Nanosci. Nanotechnol.*, 2009, **9**, 1709–1713.
16 I. Carmeli, L. Frolov, C. Carmeli and S. Richter, Photovoltaic Activity of Photosystem I-Based Self-Assembled Monolayer, *J. Am. Chem. Soc.*, 2007, **129**, 12352–12353.
17 N. Nelson and C. F. Yocum, Structure and Function of Photosystem I, *Annu. Rev. Plant Biol.*, 2006, **57**, 521–565.
18 Y. Kim, D. Shin, W. J. Chang, H. L. Jang, C. W. Lee, H. E. Lee and K. T. Nam, Hybrid Z-Scheme Using Photosystem I and $BiVO_4$ for Hydrogen Production, *Adv. Funct. Mater.*, 2015, **25**, 2369–2377.
19 H. Krassen, A. Schwarze, B. Friedrich, K. Ataka, O. Lenz and J. Heberle, Photosynthetic Hydrogen Production by a Hybrid Complex of Photosystem I and [NiFe]-Hydrogenase, *ACS Nano*, 2009, **3**, 4055–4061.
20 L. He, X. Dou, X. Li, L. Qin and S. Z. Kang, Remarkable Enhancement of the Photocatalytic Activity of ZnO Nanorod Array by Utilizing Energy Transfer Between Eosin

Y and Rose Bengal for Visible Light-Driven Hydrogen Evolution, *Int. J. Hydrogen Energy*, 2018, **43**, 15255–15261.
21 Y. Takekuma, T. Ochiai and M. Nagata, Immobilization of Rhodamine B Isothiocyanate on TiO_2 for Light Harvesting in Zinc Phthalocyanine Dye-sensitized Solar Cells, *Chem. Lett.*, 2018, **47**, 225–227.
22 K. Kawakami, M. Iwai, M. Ikeuchi, N. Kamiya and J. R. Shen, Location of PsbY in Oxygen-Evolving Photosystem II Revealed by Mutagenesis and X-ray Crystallography, *FEBS Lett.*, 2007, **581**, 4983–4987.
23 J. R. Shen and N. Kamiya, Crystallization and the Crystal Properties of the Oxygen-Evolving Photosystem II from Synechococcus Vulcanus, *Biochemistry*, 2000, **39**, 14739–14744.
24 J. R. Shen, K. Kawakami and H. Koike, Purification and Crystallization of Oxygen-Evolving Photosystem II Core Complex from Thermophilic Cyanobacteria, *Methods Mol. Biol.*, 2011, **684**, 41–51.
25 R. Nagao, A. Ishii, O. Tada, T. Suzuki, N. Dohmae, A. Okumura, M. Iwai, T. Takahashi, Y. Kashino and I. Enami, Isolation and Characterization of Oxygen-Evolving Thylakoid Membranes and Photosystem II Particles from a Marine Diatom Chaetoceros Gracilis, *Biochim. Biophys. Acta*, 2007, **1767**, 1353–1362.
26 S. Chen and K. Kimura, Synthesis of Thiolate-Stabilized Platinum Nanoparticles in Protolytic Solvents as Isolable Colloids, *J. Phys. Chem. B*, 2001, **105**, 5397–5403.
27 L. M. Utschig, N. M. Dimitrijevic, O. G. Poluektov, S. D. Chemerisov, K. L. Mulfort and D. M. Tiede, Photocatalytic Hydrogen Production from Noncovalent Biohybrid Photosystem I/Pt Nanoparticle Complexes, *J. Phys. Chem. Lett.*, 2011, **2**, 236–241.
28 S. Takeuchi, M. Takashima, M. Takase and B. Ohtani, Digitally Controlled Kinetics of Titania-Photocatalyzed Oxygen Evolution, *Chem. Lett.*, 2018, **47**, 373–376.